Theor. Appl. Climatol. 70, 65–79 (2001)

Theoretical and Applied Climatology

[1] Laboratory of Water Resources, Helsinki University of Technology, HUT, Finland
[2] Finnish Meteorological Institute, Helsinki, Finland

Test of a simple two-layer parameterisation to simulate the energy balance and temperature of a snow pack

H. Koivusalo[1], **M. Heikinheimo**[2], and **T. Karvonen**[1]

With 10 Figures

Received November 18, 1999
Revised June 17, 2000

Summary

Reasonably simple yet realistic modelling schemes simulating the heat and mass balance within a snow pack are required to provide the necessary boundary conditions for meteorological and hydrological models. An improvement to a one-layer snow energy balance model (UEB, Tarboton et al., 1995) is proposed to better simulate snow surface and snow pack temperatures and, as a result, snowmelt. The modified scheme is assessed against measured snow data from the WINTEX field campaign during spring 1997 in northern Finland, and compared with results from a complex multi-layer snow energy balance scheme. The results show that separation of a one-layer representation into two snow layers and a soil layer enables a more realistic simulation of soil and snow temperatures as well as of the snow surface temperature. The two-layer and the multi-layer snow schemes yielded comparable results for internal processes in the snow whenever the simulation was carried out under similar boundary forcing. The modified scheme is proposed for use as a sub-scheme in meteorological or hydrological models, or as a tool for simulating spatially-variable snowmelt and the surface energy balance during seasonal snow cover.

1. Introduction

The seasonal variation of snow cover has a diverse influence on hydrological and meteorological processes in high latitudes. From the hydrological point of view, the processes to be simulated are, e.g., the generation of spring snowmelt and flooding, the formation and magnitude of the snow load, and the evolution and distribution of snow depth. For meteorological purposes, surface boundary processes such as turbulent heat fluxes, net radiation and heat conduction into and within snow are important in describing the lower boundary condition for atmospheric models. The high albedo of snow in the visible portion of the solar radiation spectrum and the high emissivity of snow in the thermal part of the spectrum influence energy exchange and skin temperature at the snow surface.

A number of snow models of varying complexity are available to quantify and simulate these processes using routine meteorological data. Major differences between the models are found in the calculation of the energy to melt the snow, and in the representation of internal processes within the snow.

The energy index approach is the simplest way to approximate the energy available to melt snow. As an example, daily temperature and/or radiation have been used as an energy index to melt snow in operational models for streamflow forecasting (Vehviläinen, 1992; Rango and Martinec, 1995; Kustas et al., 1994). One of the advantages of the energy index approach is the limited data requirement, allowing applications over large areas (e.g., Bergström and Graham, 1998). The energy index approach, however, is less applicable

if separation of the snow surface energy fluxes and prediction of the surface temperature are important. A full energy balance approach becomes preferable, e.g., in coupling hydrological schemes with atmospheric circulation or weather forecasting models (Marshall et al., 1999), and in predicting the hydrological impacts of land use change, such as forest clear-cutting (Lundberg, 1996; Harding and Pomeroy, 1996).

The concepts of the snow surface energy balance have already been presented by the U.S. Army Corps of Engineers (1956), Anderson (1968), and Price and Dunne (1976). Models that simulate the surface energy balance but treat the snow pack as a bulk layer have been proposed as an efficient means of separating the components of radiation, the turbulent fluxes of latent and sensible heat, and the advected heat from precipitation (Ohta, 1994; Wigmosta et al., 1994; Tarboton et al., 1995; Stähli and Jansson, 1998). Such models are computationally relatively simple and are suggested as being well suited for modelling spatially-variable snow processes. Models that subdivide snow into horizontal layers use surface mass and energy exchange as boundary conditions to the equations of heat and mass transfer within the snow pack (Anderson, 1976; Morris, 1983; Illangasekare et al., 1990; Jordan, 1991; Tuteja and Cunnane, 1997). Such multi-layer models produce vertical profiles of density, temperature and liquid water content in the snow, and allow comparison with detailed point-measurements.

Despite of the availability of multi-layer energy balance models, there is still a need for a simple parameterisation of snow that yields consistent surface energy fluxes and skin temperature. Bergström and Graham (1998) call for the implementation of surface energy balance routines in operational continental scale rainfall-runoff models to enable a more consistent link to the climate models. The parameterization of such an energy balance scheme should not be more complex than the underlying conceptual rainfall-runoff model.

Simple energy balance schemes using a one-layer representation of the snow can successfully simulate the dominant snow processes, such as snowmelt and the major energy fluxes. However, these simple schemes may become deficient when comparing the results against measurements of liquid water content and the thermal state of the snow. Blöschl and Kirnbauer (1991) compared the capability of a simple energy budget model and a multi-layer model to simulate the internal processes in the snow. As verified with measurements, the simple model could not predict liquid-water content of the snow and the resulting snowmelt dynamics as well as the multi-layer model. The use of a layered approach was preferred in snowmelt calculation. A comparison between the one-layer model, UEB (Tarboton et al., 1995), and a multi-layer snow energy balance model, SNTHERM.89 (Jordan, 1991), was presented by Koivusalo and Heikinheimo (1999). The comparison showed that both models yielded successful mass balance calculations in terms of snow water equivalent and melt water discharge from the snow pack. Differences were found in the calculation of snow albedo and snow surface temperature, which altered the estimates of net radiation and turbulent heat fluxes, respectively. In UEB the bulk heat content of the snow and the layer of soil beneath the snow pack was combined, which made the estimation of the average snow temperature difficult. The study by Koivusalo and Heikinheimo (1999) suggested some modifications to improve the capability of the simple snow energy balance model to simulate snow temperature and heat conduction into the snow. In particular, a more realistic representation of snow requires a scheme for internal processes that separates the heat exchanges within snow and soil. The snow pack can be further divided into two layers to better account for the extremely non-linear heat exchange close to the snow surface. The upper snow layer exchanges energy with the atmosphere and shows a large variation in heat content, whereas the heat exchange in the bottom layer occurs through conduction and is reduced due to the insulating effect of the layer above.

In the present study, the suggested two-layer snow scheme is compared in terms of snow internal variables to the results of SNTHERM and to the measurements available from the WINTEX field campaign during spring 1997.

2. Site description and data

Micrometeorological and snow data (Heikinheimo et al., 2001) were measured at the Sodankylä Meteorological Observatory (67°22′ N, 26°39′ E, elevation 179 m above sea level) during the

WINTEX campaign as part of NOPEX (northern hemisphere climate processes field experiment, Halldin et al., 1999).

Sodankylä is located about 100 km north of the Arctic Circle; the climate there is subarctic and characterized by long and cold continental-type winters and relatively warm but short summers. During 1931–60 the average annual precipitation was 507 mm and the mean annual temperature −0.5 °C. Low solar elevations and short days prevail during the winter, resulting in a mostly negative radiation balance and stable atmospheric conditions.

The meteorological data from Sodankylä Observatory covered the period March 12–May 30, 1997. The data used in this study included downward short-wave radiation at a height of 16.8 m, reflected short-wave radiation at 2 m, net radiation at 2 m, both air temperature and relative humidity at 2 m, wind speed at 22 m, cloud cover observations, precipitation and form of precipitation. Radiation measurements were taken at hourly and the other meteorological data at 3-hourly intervals.

Vertical profiles of snow density and temperature were measured close to the Observatory in an opening with a diameter of about 20 m within a sparse coniferous forest stand. The height of the trees surrounding the site increases with distance from 4–6 m to 6–15 m at a distance of about 50 m. Eight thermocouples (Chromel-Constantan) were installed at fixed heights between 0.1 and 0.9 m above the ground surface to measure the temperature within the snow. Two infrared sensors (Everest Inter Sci. Inc., model 4000) were pointed downward to measure the snow surface (skin) temperature. A Campbell 21X logger automatically recorded one-minute measurements and stored hourly mean values. Snow depth, snow water equivalent, and snow density profiles were measured manually depending on the occurrence of precipitation and snowmelt, but at least once a week. The snow density profile was measured within a distance of 10–20 m from the snow temperature sensors by weighing cylindrical snow samples having a 0.1 m vertical resolution.

3. Snow models

A multi-layer snow model, SNTHERM, with detailed parameterisation of the heat processes was used as a reference to assess the results of a simpler modelling scheme. The simple scheme used the principles of UEB to derive snow surface energy exchange, but the representation of the snow and the soil was modified to overcome the problems found in Koivusalo and Heikinheimo (1999).

3.1 SNTHERM

Detailed documentation of SNTHERM.89 is given in Jordan (1991) and only some general aspects of the model are mentioned below. SNTHERM describes the heat and mass processes within the snow by subdividing the snow pack into horizontally infinite homogeneous layers, whose number increases with snow depth. The layers are subject to heat balance and mass balance equations for the three water phases and their mixture in the snow. The model accounts for the densification and metamorphosis of snow and their impact on its optical and thermal properties. The liquid water percolation through the snow is taken as a gravitational flux ignoring the effects of capillarity. The effect of freezing and melting on the mass and energy balance is coupled using a freezing curve that determines the relation between the depression temperature below 0 °C and the liquid water content in the snow. The heat balance equation accounts for the penetration of short-wave radiation into the snow pack.

Precipitation and the turbulent exchange of water vapour determine the snow surface boundary condition for mass balance. Liquid water is drained out of the snow pack at the snow/soil interface and does not enter the soil profile, where liquid water movement is disregarded. The surface boundary condition for the heat balance is set by the net radiation, by the turbulent energy exchange, and by the heat of precipitation. The snow surface albedo may either be taken as a constant, or the variable snow albedo scheme of Marks (1988) may be used. The bottom boundary condition for the heat balance is a constant temperature at the lowest soil node.

In later versions of the model the calculation of turbulent heat fluxes has been revised (e.g., Jordan, 1992). The fluxes are derived from the estimated temperature and vapour pressure gradients between the snow surface and a reference height. The bulk transfer coefficients for turbulent heat exchange are corrected for atmospheric

stability using the Richardson number as a measure of stability. The correction has been reported to degrade the model performance (Jordan, 1991) and it is suggested that the correction should be used in a restricted mode, where the Richardson number is limited to a maximum value.

SNTHERM does not account for the effects of capillary pressure on water flow, fingering flow, water ponding above ice lenses, and soil water movement. Mass changes due to vapour diffusion in the soil are ignored, except for the top soil layer when it is exposed to the air.

Case studies with SNTHERM have been reported by Koivusalo and Burges (1996), Cline (1997) and Davis et al. (1997). SNTHERM has been used as a reference model by Levine and Knox (1997) and Marshall et al. (1999).

3.2 Modifications to UEB

The details of UEB are given in Tarboton et al. (1995) and Tarboton and Luce (1996). The following outlines the model procedures, including the modifications to improve the performance of the model in predicting snow thermal properties, such as snow surface temperature and average snow temperature.

The original UEB uses a lumped representation of the snow pack plus a predefined layer of soil that interacts thermally with the snow pack. The basic state variables include snow water equivalent, snow energy content, and snow surface age. The inclusion of soil and snow heat content makes the estimation of average snow temperature difficult, which in turn affects the predictions of heat conduction into the snow and the snow surface temperature (Koivusalo and Heikinheimo, 1999). UEB was modified to separate the bulk thermal processes in the snow and the soil. The soil down to a prescribed depth was treated as a separate layer, and the snow was subdivided into two horizontally infinite layers. The two-layer snow scheme restricts the heat exchange with the atmosphere only to the upper snow layer. The lower snow layer exchanged heat through conduction with the upper snow and bottom soil layers. The depth of the top snow layer was restricted to a maximum water equivalent of snow (SWE), which was a model parameter. A snow pack having less snow than this maximum SWE was modelled as a single layer.

3.2.1 Snow energy balance

The energy balance at the snow surface is calculated as

$$M_0 = R_d - R_u + L_d - L_u + H + LE + P - Q_0, \tag{1}$$

where M_0 is the energy available to melt snow (kJ/m^{2}h), R_d is the downward short-wave radiation, R_u is the reflected short-wave radiation, L_d is the atmospheric long-wave radiation, L_u is the upward long-wave radiation, H is the sensible heat flux, LE is the latent heat flux, P is the advective heat from precipitation, and Q_0 is the heat conduction to the top snow layer. Positive energy flux is directed towards the snow. Under freezing conditions ($M_0 = 0$), the snow surface temperature is iterated by balancing the atmospheric energy fluxes with the heat conduction into the snow. After the snow surface temperature reaches 0 °C, the net energy input M_0 is used to melt snow in the upper snow layer. The heat balance of a snow layer is calculated as:

$$\frac{dU_j}{dt} = Q_{j-1} - Q_j + M_{j-1} - M_j, \qquad j = 1, 2 \tag{2}$$

where U_j is the heat content of the snow layer j (kJ/m^2), Q_j is the heat conduction between layers j and $j+1$ (kJ/m^2 h), and M_j is the energy advected with meltwater outflow from layer j to $j+1$. In the present two-layer snow model $j = 1$ and $j = 2$ refer to the upper and lower snow layers, respectively. The heat content of the snow is defined relative to a reference state of water at 0 °C in the ice phase. The relationship between the heat content, the average temperature and the liquid water content of the snow layer is (Tarboton et al., 1995):

$$U_j = \begin{cases} T_j C_i W_j \rho_w & T_j < 0,\ L_{f,j} = 0 \\ L_{f,j} h_f W_j \rho_w & T_j = 0, L_{f,j} \geq 0, \end{cases} \tag{3}$$

where T_j is the average snow temperature in layer j (°C), C_i is the specific heat of ice (2.09 kJ/kg °C), W_j is the water equivalent of the snow (m), ρ_w is the density of water (1000 kg/m^3), $L_{f,j}$ is the mass fraction of liquid water in layer j, and h_f is the latent heat of fusion (333.5 kJ/kg).

To obtain a more realistic simulation of the heat conduction in the snow, snow density was added to the model as a state variable, and an effective

thermal conductivity of snow was used as in Anderson (1976):

$$k_T = a_T + b_T(\rho_s/\rho_w)^{c_T}, \tag{4}$$

where k_T is the thermal conductivity of snow (kJ/h m °C), a_T, b_T, and c_T are parameters (0.0756 kJ/h m °C, 9.036 kJ/h m °C, and 2.0), and ρ_s is the density of the snow. The heat conduction between the snow layers was calculated explicitly from the estimated temperature gradient:

$$Q_j = -\overline{k_T}\frac{T_{j+1} - T_j}{\Delta z_{j,j+1}}, \tag{5}$$

where Q_j is the heat conduction from layer j to layer $j+1$, and $\Delta z_{j,j+1}$ is the distance between the midpoints of layers j and $j+1$. The thermal conductivity $\overline{k_T}$ between the layers was estimated as:

$$\overline{k_T} = \frac{\Delta z_j + \Delta z_{j+1}}{\Delta z_j/k_T^j + \Delta z_{j+1}/k_T^{j+1}}, \tag{6}$$

where k_T^j is the thermal conductivity in layer j.

Liquid water percolation in snow is assumed to occur at 0 °C and the heat of meltwater is given relative to the ice phase:

$$M_j = F_j\rho_w h_f \tag{7}$$

where F_j is the water outflow from layer j to $j+1$ (m/h).

3.2.2 Snow mass balance

The snow mass balance was calculated in the same way as in Tarboton et al. (1995). The mass input at the snow surface is written:

$$F_0 = P_r + P_s - E, \tag{8}$$

where F_0 is the atmospheric mass forcing at the snow surface (m/h), P_r is the liquid precipitation, P_s is the solid precipitation, and E is evaporation/sublimation. The mass balance of a snow layer becomes:

$$\frac{dW_j}{dt} = F_{j-1} - F_j, \tag{9}$$

$$F_j = K_{\text{sat}}S_j^3, \quad j = 1, 2, \tag{10}$$

$$S_j = \frac{L_{f,j}/(1 - L_{f,j}) - L_c}{\rho_w/\rho_s - \rho_w/\rho_i - L_c}, \tag{11}$$

where W_j is the snow water equivalent (liquid plus ice in m), F_j is the water outflow from layer j to $j+1$ (m/h), K_{sat} is the saturated hydraulic conductivity (20 m/h), S_j is the relative saturation in excess of water retained by capillary forces, L_c is the liquid water retention capacity (0.05), and ρ_i is the density of ice (917 kg/m^3). The meltwater outflow is discharged from the snow at the ground surface and does not enter the soil.

The snow density changes in two stages due to snow compaction and metamorphism (Anderson, 1976; Jordan, 1991):

$$\frac{d\rho_s^j}{dt} = \rho_s^j\left(c_1 W^* e^{-c_2(T^* - T_j)}e^{-c_3\rho_s^j}\right), \tag{12}$$

$$\frac{d\rho_s^j}{dt} = \rho_s^j\left(c_4 e^{-c_5(T^* - T_j)}c_6\right), \tag{13}$$

$$c_6 = e^{-c_7(\rho_s^j - \rho_d)}, \qquad \rho_s^j > \rho_d, \tag{14}$$

$$c_6 = 1, \qquad \rho_s^j \le \rho_d, \tag{15}$$

where c_1, c_2, and c_3 are parameters (1.0 1/m h, 0.08 1/°C, 0.021 m^3/kg), ρ_s^j is the density of the snow in layer j (kg/m^3), W^* is the load of snow water equivalent (snow in the layer above and 50% of the snow in the current layer), c_4, c_5, and c_7 are parameters (0.01 1/h, 0.04 1/°C, 0.046 m^3/kg), ρ_d is 150 kg/m^3, and T^* is 0 °C. The density change in Eq. (13) is enhanced by a factor of 2 when liquid water is present in the snow. The density of new snow (kg/m^3) is calculated as a function of air temperature:

$$\rho_{ns} = \begin{cases} 50 & T \le -15\,^\circ\text{C} \\ 50 + 1.7(T + 15)^{1.5} & T > -15\,^\circ\text{C}, \end{cases} \tag{16}$$

3.2.3 Soil heat balance

The heat content of a soil layer is defined as in Karvonen (1988):

$$U_g = (1 - \phi)D_g\rho_g C_g T_g + wD_g\rho_w C_w T_g + ID_g\rho_i C_i T_g - ID_g\rho_i h_f, \tag{17}$$

where U_g is the heat content of the soil (kJ/m^2), T_g is the average soil temperature (°C), w is the liquid water content, I is the ice content, ϕ is the porosity of the soil, C_g is the specific heat of the soil (kJ/kg °C), C_w is the specific heat of water, ρ_g is the density of the soil grains (kg/m^3), and D_g is the depth of the soil layer (m). The water movement in the soil was disregarded and the total water content of the soil was assumed constant.

The soil heat and mass balances were related by using a freezing depression curve:

$$w = (w + I)e^{-(T_f - T_g)/d_g}, T_g < 0\,^{\circ}\mathrm{C}, \quad (18)$$

where T_f is the freezing point temperature, and d_g is a parameter (0.5...1.5 in sandy soils). Combining Eqs. (17) and (18) defines a relationship between soil heat and liquid water content. The soil temperature can be solved by iterative methods when the soil heat content is known. The heat conduction from the bottom snow layer to the soil was calculated according to Eq. (5) with the estimated temperature gradient between the bottom snow layer and the soil, and the assumed constant thermal conductivity of the soil.

3.2.4 Surface energy fluxes

The energy fluxes at the snow surface determine a boundary condition for the energy balance of the upper snow layer. In this study, the net short-wave radiation and the downward long-wave radiation were taken as inputs to the model. The upward long-wave radiation is calculated as a function of the snow surface temperature according to the Stefan–Boltzman law:

$$L_u = \varepsilon_s \sigma (T_0 + 273.15)^4 + (1 - \varepsilon_s) L_d, \quad (19)$$

where ε_s is the emissivity of snow (0.97), σ is the Stefan–Boltzmann constant ($2.04 \cdot 10^{-7}$ kJ/m^2 h K^4), and T_0 is the snow surface temperature (°C).

The bulk transfer coefficients for the calculation of turbulent heat fluxes are estimated by assuming a logarithmic wind profile above the snow surface and equal exchange coefficients for momentum, heat and vapour transfer:

$$K_N = \frac{k^2 u}{[\ln(z/z_0)]^2}, \quad (20)$$

where K_N is the bulk transfer coefficient (m/h) for momentum, heat or water vapour in neutral atmospheric stability, k is von Karman's constant, u is the wind speed (m/h) measured at the reference height of z, and z_0 is the roughness length (m). Tarboton et al. (1995) used a correction for stable and unstable atmospheric stability following Price and Dunne (1976):

$$K_* = K_N/(1 + 10Ri), \quad \text{stable } Ri > 0, \quad (21)$$

$$K_* = K_N(1 - 10Ri), \quad \text{unstable } Ri < 0, \quad (22)$$

$$Ri = \frac{g(T_a - T_0)z}{u^2[0.5(T_a + T_0) + 273.15]}, \quad (23)$$

where K_* is the bulk transfer coefficient, Ri is an estimate of the Richardson number, and g is the acceleration due to gravity. Tarboton and Luce (1996) introduced an interpolation scheme to restrict the strength of the correction, because the corrected bulk transfer coefficients gave unreasonable values with large temperature differences between the reference height and the snow surface. A comparison between the turbulent flux scheme of UEB with that of SNTHERM reveals that a major difference between the methods is the inclusion of the free convection coefficient in SNTHERM (Jordan, 1992). The calculation of the turbulent heat fluxes was modified in the two-layer scheme to account for the flux due to the windless convection of sensible heat:

$$H = (K_* \rho_a c_p + C_{sk})(T_a - T_0), \quad (24)$$

$$LE = K_* h_v \frac{0.622 \rho_a}{P_a}[e_a - e_s(T_0)], \quad (25)$$

where H is the sensible heat flux (kJ/m^2 h), ρ_a is the air density, c_p is the heat capacity of air (1.005 kJ/kg °C), C_{sk} is the windless convection coefficient for the sensible heat flux (7.2 kJ/m^2 h °C), LE is the latent heat flux (kJ/m^2 h), P_a is the atmospheric pressure (Pa), e_a is the air vapour pressure, e_s is the saturated vapour pressure at the snow surface, and h_v is the latent heat of sublimation of ice (2834 kJ/kg). When the snow surface temperature is 0 °C, h_v is taken as the latent heat of vaporization of water (2500.5 kJ/kg).

The advected heat from precipitation was calculated as the energy needed to convert precipitation to the ice phase at 0 °C.

4. Model setup

4.1 Input data

The models used identical input data which included net short-wave radiation, downward long-wave radiation, air temperature, relative humidity, wind speed, and precipitation. All the variables were measured or estimated at a height of 2 m. Koivusalo and Heikinheimo (1999) studied the Sodankylä dataset of spring 1997 and estimated the effect of the forest canopy on the downward short-wave radiation and the wind speed as described below.

Since the short-wave radiation was measured above the canopy at a height of 16 m, the short-wave radiation input near the snow surface was derived from the existing measurements of net all-wave radiation and reflected short-wave radiation at a height of 2 m, and from the estimated net long-wave radiation. The procedure implemented in SNTHERM was used to estimate the downward long-wave radiation, and the measured snow surface temperature was used to calculate the upward thermal radiation.

The wind speed was measured at a height of 22 m and the corresponding value at a height of 2 m was estimated by linearly reducing the wind speed by 68%. This reduction was based on observations during the turbulent flux measurements, when the vertical wind profile within the sparse canopy was approximately linear.

The forest surrounding the site plays a role in the snow surface energy balance through canopy shading effects, through the emission of long-wave radiation and through the effects of the canopy on turbulent transfer. In this study, the effect of the canopy on incoming short-wave radiation and wind speed was accounted for, but the effects of the forest canopy on long-wave radiation and turbulent transfer coefficients were ignored.

4.2 Model parameters

The values of the parameters for SNTHERM were as suggested in the model documentation except for the roughness length, which was set to a value of 0.005 m as suggested in the UEB documentation. In the calculation of the bulk transfer coefficients, the two-layer scheme was made similar to SNTHERM by implementing a correction for the weak transfer of sensible heat. The documentation of the original UEB did not suggest any correction for atmospheric stability, but the correction was used in this study as implemented in Eqs. (21–22). The correction in SNTHERM was according to the suggestion in the model documentation, i.e., a stability correction was used by setting an upper limit (0.16) on the Richardson number. In this paper the turbulent fluxes from SNTHERM were used as a reference. The fluxes from SNTHERM were verified against eddy-correlation measurements in an earlier study by Koivusalo and Heikinheimo (1999).

Table 1. Soil parameters for the two-layer snow scheme

Parameter	Description	Value
ϕ	soil porosity	0.4
θ	soil moisture content	0.2
ρ_g	density of soil grains	2700 kg/m^3
c_g	heat capacity of soil	1.5 kJ/kg °C
k_g	thermal conductivity of soil	2.0 kJ/m °C/h
d_g	parameter in freezing curve	1.5
D_g	depth of active soil layer	0.4 m

The maximum mass of the upper snow layer was a new parameter introduced when the snow representation of UEB was modified. This parameter was set to a value of 0.02 m. The soil parameters were set as given in Table 1 and followed the ranges given in the literature. The ground heat flux at the bottom of the soil layer was assumed to be zero. To correct for the underestimation of the gauge, precipitation was increased by a factor of 1.3 for snowfall and 1.15 for mixed rain and snow. The air pressure was set to a constant value of 99 kPa.

Results from UEB are shown for comparison, and are taken from Koivusalo and Heikinheimo (1999). They used UEB with the parameter values suggested in the model documentation, and therefore no correction for atmospheric stability was used.

5. Results and discussion

5.1 Net long-wave radiation and turbulent heat fluxes

The accumulated net long-wave radiation during spring 1997 calculated by the two-layer scheme, SNTHERM, and UEB is shown in Fig. 1. The net fluxes by the two-layer scheme and SNTHERM were practically the same, while UEB yielded a higher net loss of long-wave radiation during late winter, which was due to the different simulated surface temperature of the snow. The net short-wave and downward long-wave radiation were used as an input to all the schemes.

Figure 2 shows that the cumulative flux of sensible heat calculated by the two-layer scheme was slightly higher than the flux by SNTHERM. The difference between the calculated fluxes can be considered relatively small and has no significant effect on the snow mass balance. The

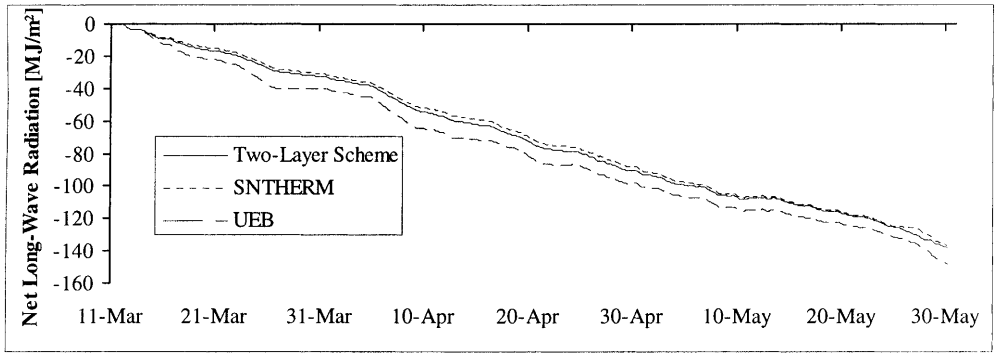

Fig. 1. Calculated cumulative net long-wave radiation during spring 1997 in Sodankylä. The results of the two-layer scheme were practically the same as those of SNTHERM. The downward long-wave radiation was used as an input to the models. Negative flux is directed away from the snow

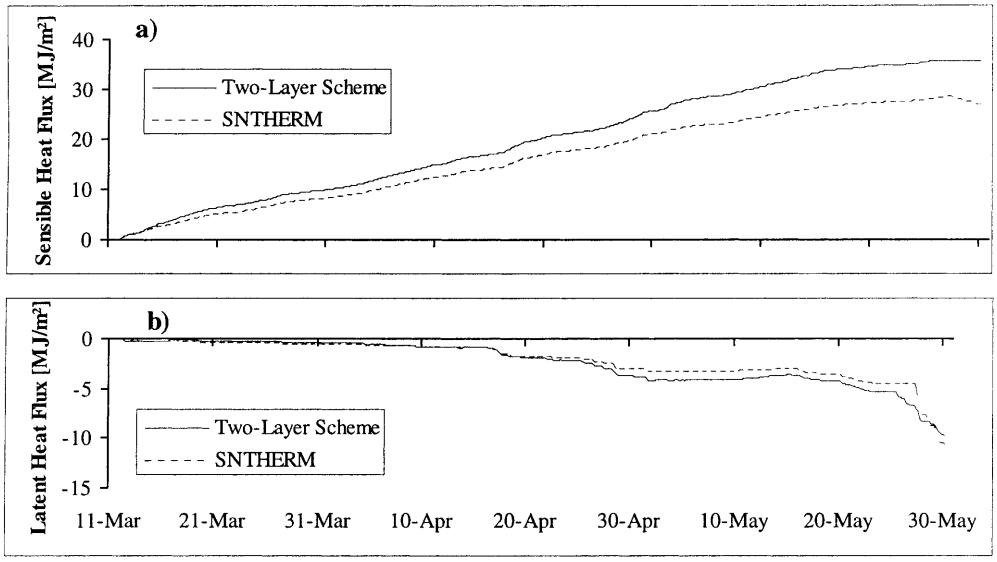

Fig. 2. Calculated cumulative fluxes of sensible heat (**a**) and latent heat (**b**) during spring 1997 in Sodankylä. Positive flux is directed towards the snow

sensible heat flux was sensitive to the roughness length and to the inclusion of the correction scheme for atmospheric stability. The absolute magnitude of the latent heat flux was small and similar for each of the models when the ground was snow-covered. The magnitude of the advected heat from precipitation was insignificant in both of the model runs.

Figures 1–2 show that the two-layer scheme and SNTHERM had nearly identical boundary conditions (similar energy fluxes) at the snow surface, which allows a consistent comparison of the modelled internal processes presented in the following subsections.

5.2 Snow temperature

The average snow and soil temperatures obtained from the model simulations and the measurements are shown in Fig. 3. The measured snow temperatures from different heights within the snowpack were averaged to obtain the mean snow temperature comparable with the model outputs. The results of SNTHERM and the two-layer scheme were the average temperature weighted by the depth of the snow layers. The result obtained from UEB was a temperature index of the snow and soil derived directly from the calculated heat content, and thus was not directly comparable to

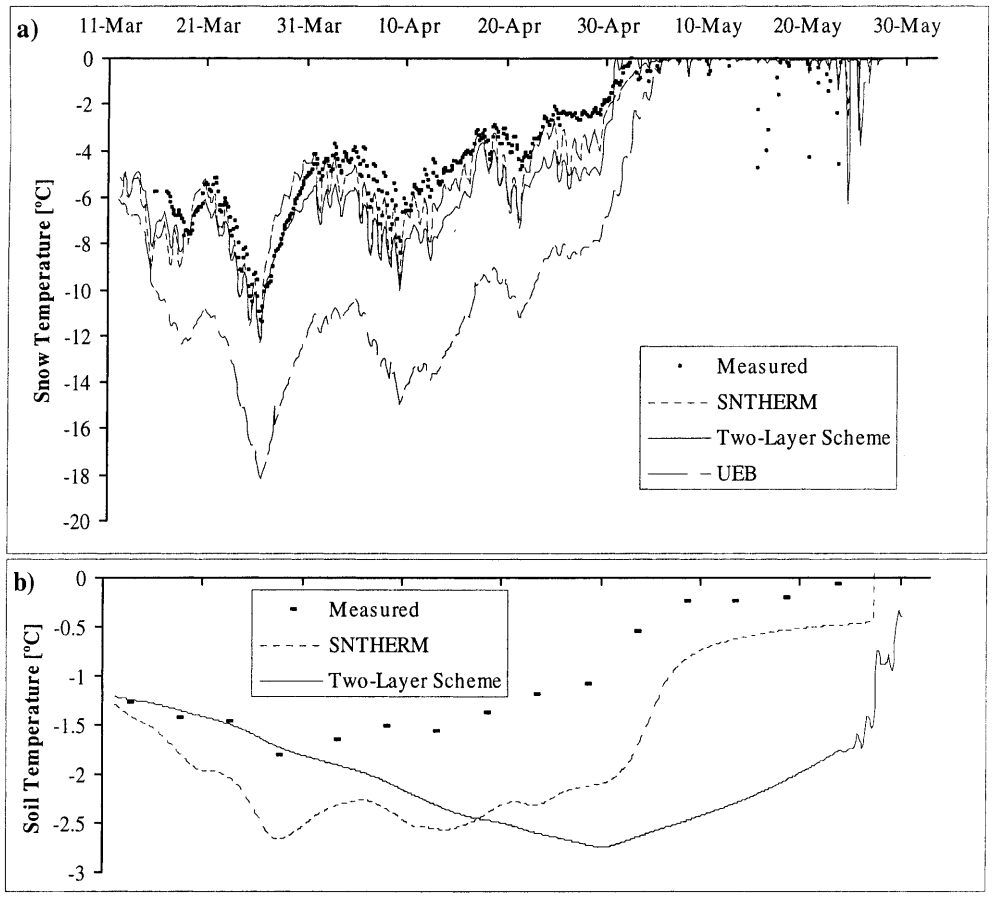

Fig. 3. Measured and calculated average temperatures of snow (**a**) and soil (**b**) during spring 1997. The measured snow temperature was the average of temperature sensors located within the snow pack. The result of SNTHERM and the two-layer scheme were snow-depth averaged temperatures. The result of UEB was a temperature index of the snow and soil layer

the measurements. SNTHERM yielded a slightly lower average temperature compared to the measurements. The results of the two-layer scheme showed lower temperatures than SNTHERM, which was due to differences in the predicted soil temperature. The average temperature of the top 0.4 m of soil varied little during the calculation period and compared well with the SNTHERM results and moderately with the two-layer scheme.

The heat content simulated by the two-layer scheme was slightly less than that simulated by SNTHERM during the winter, while the maximum heat content was slightly greater than that calculated using SNTHERM (Fig. 4). The difference was due to the discrepancy in the modelled

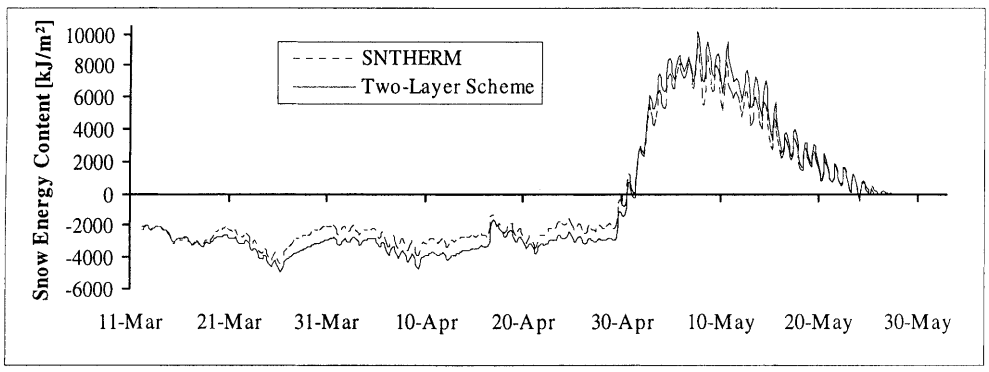

Fig. 4. Calculated total heat content of the snow by SNTHERM and by the two-layer scheme during spring 1997

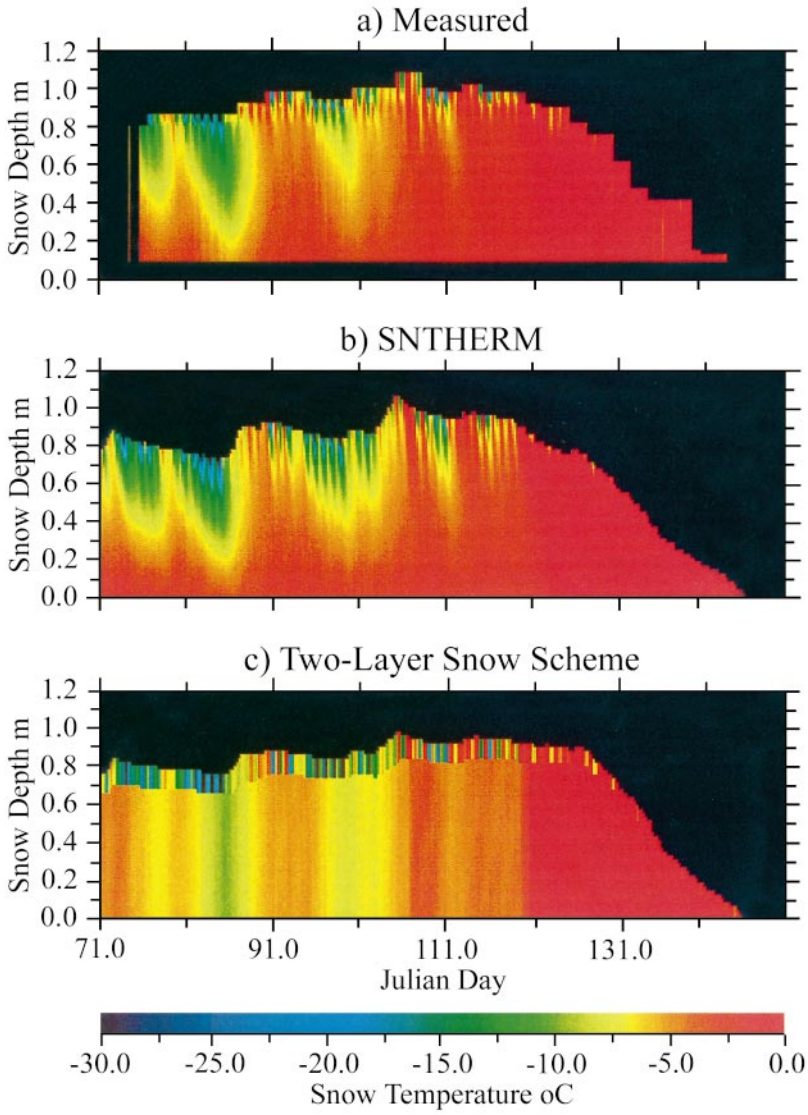

Fig. 5. Calculated and measured time evolution of snow temperature profiles during spring 1997. The measured values (**a**) were interpolated linearly from point measurements made with a 10 cm resolution in the snow and from the measured surface temperature of the snow. The SNTHERM results (**b**) were interpolated from the model output of snow layer temperatures. The results of the two-layer scheme (**c**) show the predicted bulk temperatures for the snow layers. The temporal resolution of the graphs is 6 hours and the vertical resolution 0.02 m

soil temperature and to the effect of nonlinear heat exchange within the snow.

Figure 5 illustrates the evolution of the simulated and measured snow temperature structure during spring 1997. The measured profile was interpolated linearly from the point measurements made at 10 cm intervals in the snow. The SNTHERM results were interpolated from the detailed model output of snow layer temperatures. For the two-layer scheme the simulated bulk temperatures of the upper and lower snow layers are shown. The temperature profiles illustrate the cooling of the snow surface and the resulting nonlinear temperature profile below the surface during cold nights. The temperature predicted by SNTHERM shows slightly lower night-time temperatures than those measured near the snow surface. The differences were sensitive to the predicted snow depth. The two-layer scheme demonstrated the difficulties of predicting a nonlinear temperature profile using only two layers. The temperature of the top layer matched well with the SNTHERM results close to the surface, whereas the temperature of the bottom snow layer was close to the measured temperature in the middle of the snow pack. The time of the occurrence of isothermal snow at 0 °C was well predicted by both of the models.

5.3 Snow surface temperature

The simulation error in the snow surface temperature as a function of measured temperature is shown in Fig. 6. The results of both SNTHERM

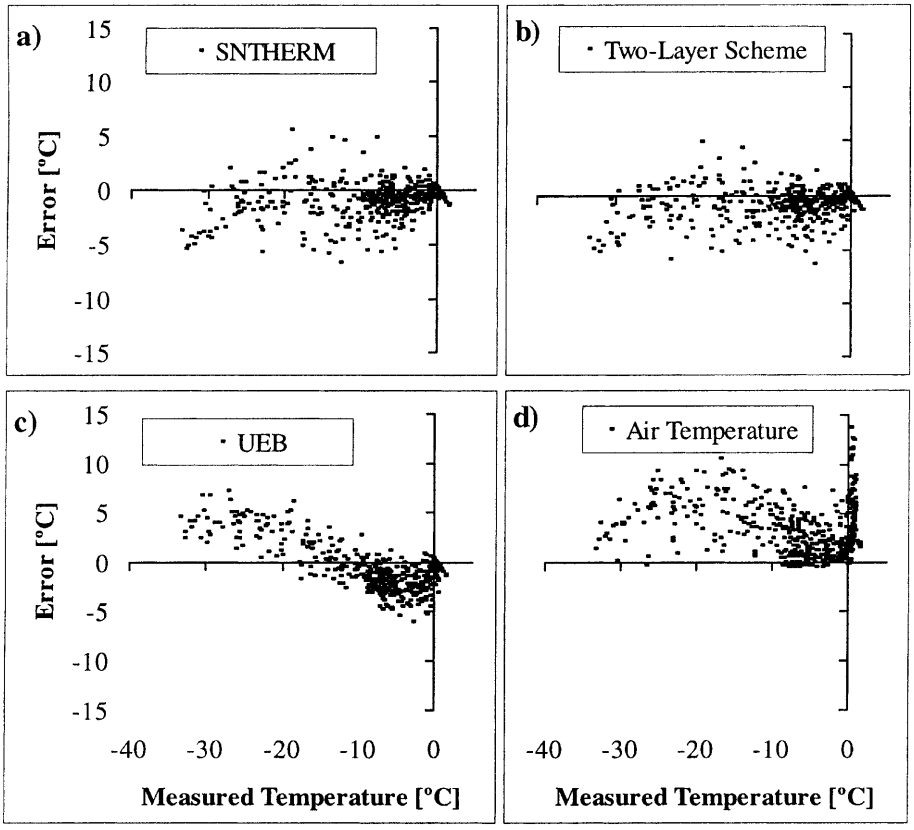

Fig. 6. Scatter graphs of simulation error versus measured snow surface temperature during 17 Mar–20 May, 1997. The results of SNTHERM, the two-layer scheme, and UEB are shown in **a**, **b**, and **c**. Figure **d** shows the simulation error when the surface temperature is assumed equal to the air temperature

and the two-layer scheme showed a similar random scatter, whereas UEB tended to overpredict low nighttime temperatures and underpredict daytime temperatures. However, the UEB prediction could be improved by a calibration of the surface conductance parameter, which was not carried out in this or in the previous study by Koivusalo and Heikinheimo (1999). The mean temperature simulation error and its standard deviation during 17 Mar–20 May 1997 were −0.85 °C and 1.5 °C, respectively, using SNTHERM, −0.84 °C and 1.4 °C using the two-layer scheme, and −0.63 °C and 2.3 °C using UEB. If the snow surface temperature was assumed to be equal to the measured air temperature at a height of 2 m above the ground, the mean error and standard deviation would be 3.2 °C and 2.8 °C. This comparison of errors suggests that the model predictions are relatively close to each other.

The nocturnal surface temperature of the snow was sensitive to the inclusion of the windless exchange of sensible heat flux and to the estimated heat conduction into the snow. The use of the windless convection coefficient improved the simulation of low surface temperatures during strong radiative cooling. The results of SNTHERM showed a steep temperature gradient near the snow surface, which we tried to replicate using a relatively thin upper snow layer in the two-layer snow scheme. The inclusion of a number of snow layers, such as in SNTHERM, improves the calculation of heat conduction during nonlinear vertical temperature profiles.

5.4 Snow mass and liquid water in snow

The mass balance in terms of the cumulative precipitation, and the calculated depth and water equivalent of snow is presented together with the measured range of the variables in Fig. 7. The two-layer scheme predicted a slightly faster snowmelt than SNTHERM, especially during the first half of the melting period. The snow depth and snow pack densification simulated by the two-layer scheme during March and April were well in accordance with the measurements and the

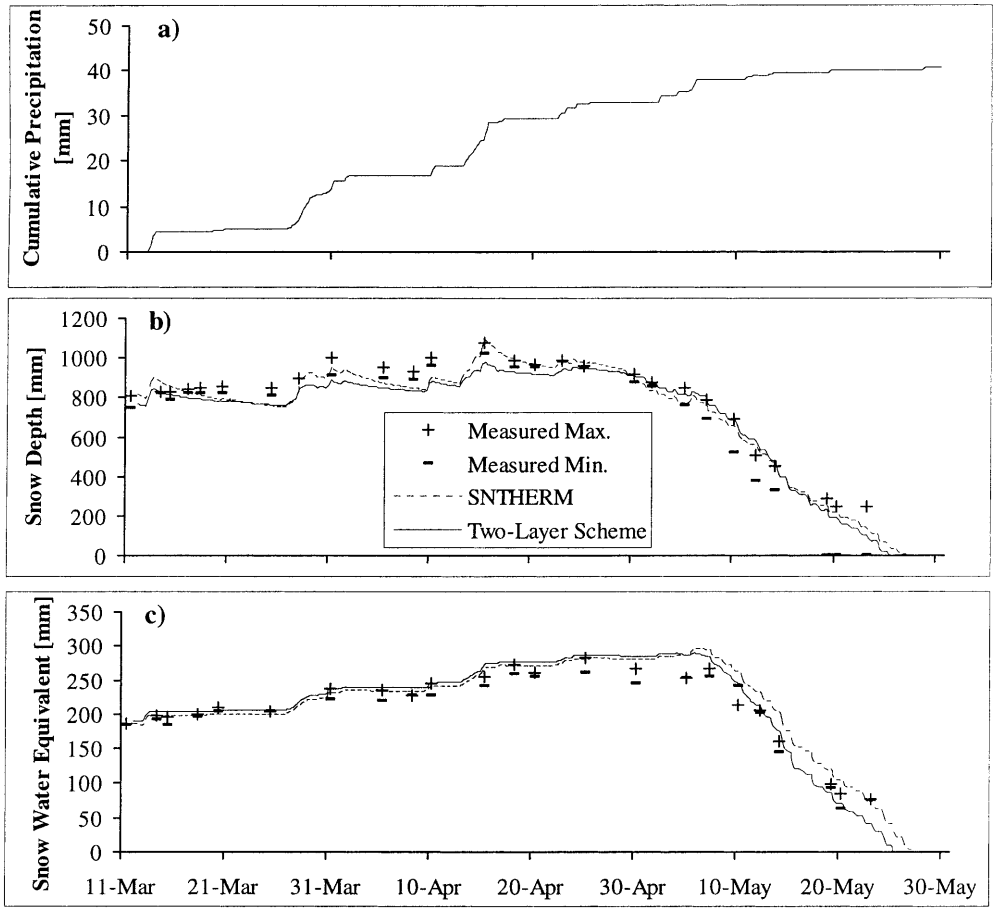

Fig. 7. Cumulative precipitation (**a**), snow depth (**b**), and snow water equivalent (**c**) calculated by SNTHERM and the two-layer scheme during spring 1997. The measured depth and water equivalent of the snow are plotted as a range between maximum and minimum values

SNTHERM results. The results of the original UEB are not shown in Fig. 7, but they were very close to the results of the two-layer scheme.

The calculated depth of liquid water retained in the snow is shown in Fig. 8. The results of the two-layer scheme are close to those of SNTHERM, except during 8–14 May when the two-layer scheme predicts a faster melt than SNTHERM. The original UEB yields liquid water in snow only after the combined layer of snow and soil reach an average temperature of 0 °C. Figure 9 shows the cumulative water flow out of the snow pack as calculated by the models. Since the two-layer scheme yielded a slightly faster snowmelt

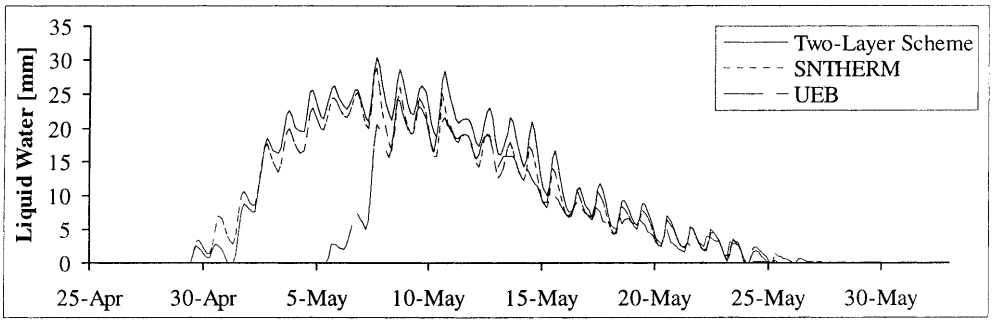

Fig. 8. Liquid water mass calculated by SNTHERM, the two-layer scheme, and UEB during the spring melt of 1997. The liquid water mass is expressed in mm of water

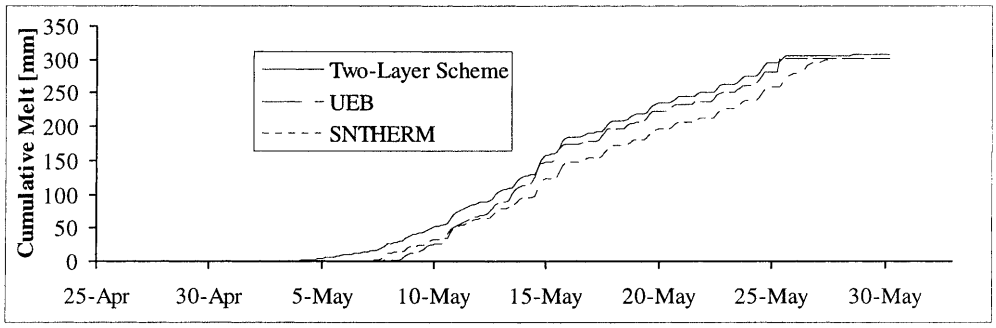

Fig. 9. Cumulative water flow out of the snow pack calculated by SNTHERM, the two-layer scheme, and UEB

than SNTHERM, the outflow starts and stops earlier. UEB resulted in a slightly faster melt that started approximately at the same time as that from SNTHERM. The average and maximum melt during May were 0.48 mm/h and 3.1 mm/h, respectively, for SNTHERM, 0.44 mm/h and 3.3 mm/h for the two-layer scheme, and 0.43 mm/h and 6.5 mm/h for UEB. UEB produced its maximum melt value at the time when the snow pack disappeared, after all the remaining snow was melted during one time step. The maximum melt for UEB that coincided with the other models was 4.0 mm/h.

5.5 Snow density

Figure 10 presents the measured and calculated time evolution of the snow density structure. The measured profile of snow bulk density (liquid + ice) was interpolated from the measurements taken once or twice a week as described in Section 2. The SNTHERM results were interpolated from the detailed model output of snow layer density (liquid + ice). The results of the two-layer scheme show the predicted bulk snow density in the upper and lower snow layers. Before the snowmelt period both measurements and model results showed less dense layers of snow near the snow surface and denser ones in the middle and at the bottom of the snow pack, which is also reproduced moderately well using the two-layer scheme. The measurements indicate that the bottom of the snow pack was less dense than the middle layers, which was not predicted by the models. Another discrepancy between the measurements and the model results was the measured major densification of snow during the snowmelt that occurred near the snow surface, in contrast to the modelled densification of the bottom of the snow pack during the percolation of liquid water. The measurements suggested that some snow layers near the surface were thick and dense enough to prevent percolation of melt water. The existence of such dense layers may also explain the persistent low density at the bottom of the snow pack before the snowmelt period.

6. Conclusions

A two-layer snow energy balance scheme was formulated by modifying an existing one-layer snow model (UEB, Tarboton et al., 1995). The modifications introduced had only minor effects on the calculated bulk SWE and snow melt, but improved the results of snow heat balance and liquid water content.

The prediction of the snow surface temperature was sensitive to the estimated turbulent heat fluxes and to the calculation of heat conduction within the snow. The results of the two-layer model in this respect were improved after a correction scheme similar to that implemented in SNTHERM was used for atmospheric stability, and after the heat conduction into the snow was described realistically by approximating the temperature gradient between the snow surface and a thin top layer of snow. The similar surface temperature produced by the two models resulted in nearly identical forcing to simulate internal processes within the snow.

The use of two snow layers was successful in representing the average vertical structure of snow temperature and snow density. Neither the multilayer nor the two-layer snow scheme could replicate the measured structure of snow density, which was presumably influenced by layers preventing water percolation through the snow. Separation of the snow and soil thermal processes

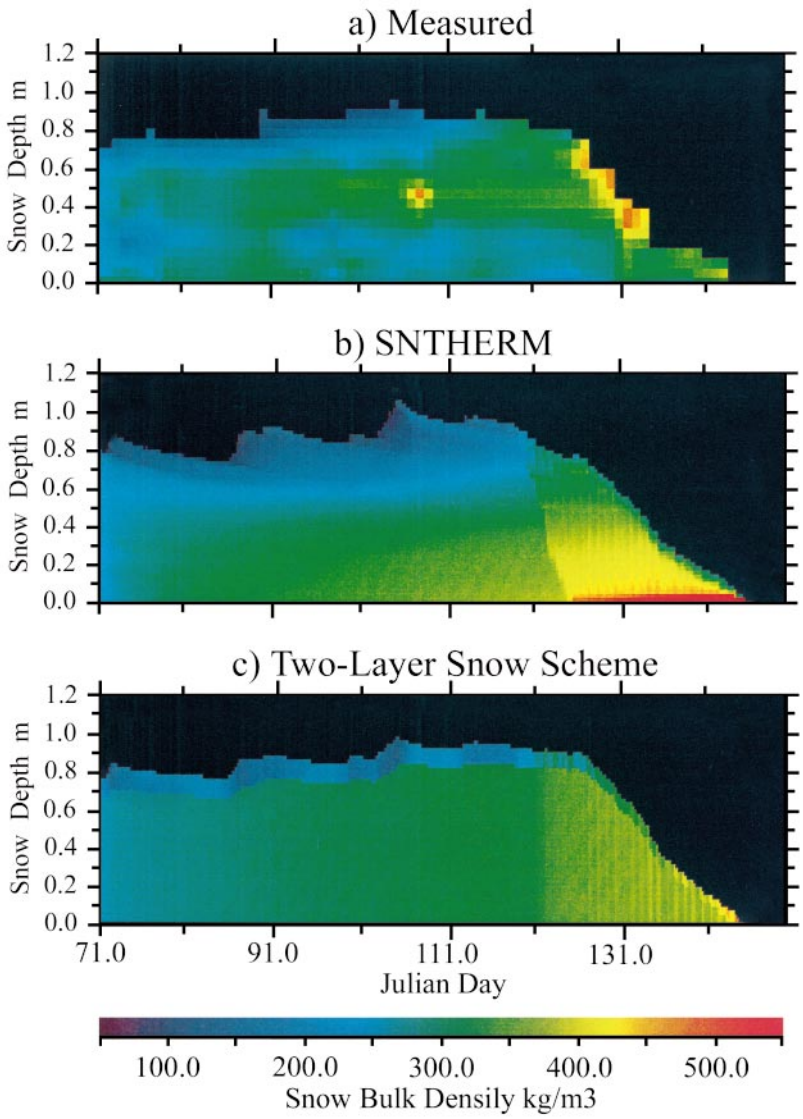

Fig. 10. Measured and calculated time evolution of snow density. The measured profile (**a**) was interpolated from the results of sampling once or twice a week. The results of SNTHERM (**b**) were interpolated from the detailed model output of snow layer density. The results of the two-layer scheme (**c**) show the bulk snow density in the upper and lower snow layers. The temporal and spatial resolutions of interpolation were 6 h and 0.02 m, respectively

was necessary to realistically simulate average snow and soil temperatures and heat content. This approach also improved the simulation of liquid water in the snow. In conclusion, the two-layer scheme and SNTHERM yielded comparable results whenever the simulation was carried out under similar boundary forcing.

Acknowledgements

This work has partly been carried out within the framework of NOPEX-WINTEX – land-surface-atmosphere interactions in a wintertime boreal landscape. Thanks are due to Timo Pirttijärvi for the snow density data, and to Rachel Jordan, David Tarboton and Charles Luce for making their snow models available. The first author acknowledges funding from the Land and Water Technology Foundation, the Finnish Cultural Foundation, and the Vilho, Yrjö and Kalle Väisälä Foundation. Support and ideal working facilities provided by Pertti Vakkilainen are appreciated.

References

Anderson EA (1968) Development and testing of snow pack energy balance equations. Water Resour Res 4: 19–37

Anderson EA (1976) A point energy and mass balance model of a snow cover. NOAA Technical Report NWS 19, 150 pp

Bergström S, Graham LP (1998) On the scale problem in hydrological modelling. J Hydrol 211: 253–265

Blöschl G, Kirnbauer R (1991) Point snowmelt models with different degrees of complexity – internal processes. J Hydrol 129: 127–147

Cline DW (1997) Snow surface energy exchanges and snowmelt at a continental, midlatitude Alpine site. Water Resour Res 33: 689–701

Davis RE, Hardy JP, Ni W, Woodcock C, McKenzie JC, Jordan R, Li X (1997) Variation of snow cover ablation in the boreal forest: A sensitivity study on the effects of conifer canopy. J Geophys Res 102(D24): 29389–29395

Halldin S, Gryning S-E, Gottschalk L, Jochum A, Lundin L-C, Van de Griend AA (1999) Energy, water and carbon exchange in a boreal forest landscape – NOPEX experiences. Agric Forest Meteor 98–99: 5–29

Harding RJ, Pomeroy JW (1996) The energy balance of the winter boreal landscape. J Climate 9: 2778–2787

Heikinheimo M, Kangas M, Koivusalo H (2001) Characteristics of the snow pack and lower atmosphere during CFE3 in sodankylâ. Theor Appl Climatol 70: Documented dataset on appended CD

Illangasekare TH, Walter RJ Jr, Meier MF, Pfeffer WT (1990) Modeling of meltwater infiltration in subfreezing snow. Water Resour Res 26(5): 1001–1012

Jordan R (1991) A one-dimensional temperature model for a snow cover: Technical documentation for SNTHERM.89, Special Report 91-16, US Army Cold Regions Research and Engineering Laboratory, Hanover, NH, 49 pp

Jordan R (1992) Estimating turbulent transfer functions for use in energy balance modeling, Internal Report 1107, US Army Cold Regions Research and Engineering Laboratory, Hanover, NH, 13 pp

Karvonen T (1988) A model for predicting the effect of drainage on soil moisture, soil temperature and crop yield, Helsinki University of Technology, Publications of the Laboratory of Hydrology and Water Resources Engineering, 1/1988, 215 p

Koivusalo HJ, Burges SJ (1996) Use of a one-dimensional snow cover model to analyze measured snow depth and snow temperature data from Southern Finland, University of Washington, Water Resources Series, Technical Report 150, 109 pp

Koivusalo H, Heikinheimo M (1999) Surface energy exchange over a boreal snowpack: comparison of two snow energy balance models. Hydrol Process 13(14–15): 2395–2408

Kustas WP, Rango A, Uijlenhoet R (1994) A simple energy budget algorithm for the snowmelt runoff model. Water Resour Res 30: 1515–1527

Levine ER, Knox RG (1997) Modeling soil temperature and snow dynamics in northern forests. J Geophys Res 102(D24): 29407–29416

Lundberg A (1996) Interception Evaporation, Processes and Measurement Techniques, Doctoral Thesis, Luleå Univ Technology Div Water Res Eng 196 D, 24 pp

Marks D (1988) Climate, Energy Exchange, and Snowmelt in Emerald Lake Watershed, Sierra Nevada, University of California, Santa Barbara, 149 pp

Marshall S, Oglesby RJ, Maasch KA, Bates GT (1999) Improving climate model representations of snow hydrology, Environmental Modelling & Software 14: 327–334

Morris EM (1983) Modelling the flow of mass and energy within a snow pack for hydrological forecasting. Ann Glaciol 4: 198–203

Ohta T (1994) A distributed snowmelt prediction model in mountain areas based on an energy balance method. Ann Glaciol 19: 107–113

Price AG, Dunne T (1976) Energy balance computations of snowmelt in a subarctic area. Water Resour Res 12: 686–694

Rango A, Martinec J (1995) Revisiting the degree-day method for snowmelt computations. Water Resour Bull 31: 657–669

Stähli M, Jansson P-E (1998) Test of two SVAT snow submodels during different winter conditions. Agric Forest Meteor 92: 31–43

Tarboton DG, Luce CH (1996) Utah Energy Balance Snow Accumulation and Melt Model (UEB), Computer model technical description and users guide, Utah Water Research Laboratory and USDA Forest Service Intermountain Research Station

Tarboton DG, Chowdhury TG, Jackson TH (1995) A Spatially Distributed Energy Balance Snowmelt Model. In: Tonnessen KA, Williams MW, Tranter M (eds) Biogeochemistry of Seasonally Snow-Covered Catchments. Proceedings of a Boulder Symposium, July 3–14, IAHS Publ no 228, 141–155

Tuteja NK, Cunnane C (1997) Modelling coupled transport of mass and energy into the snow pack – model development, validation and sensitivity analysis. J Hydrol 195: 232–255

US Army Corps of Engineers (1956) Snow Hydrology, Summary Report of the Snow Investigations, North Pacific Division, Portland Oregon, 437 pp

Vehviläinen B (1992) Snow Cover Models in Operational Watershed Forecasting, Publications of Water and Environment Research Institute 11, National Board of Waters and the Environment, Finland, 112 pp

Wigmosta MS, Vail LW, Lettenmaier DP (1994) A distributed hydrology-vegetation model for complex terrain. Water Resour Res 30: 1665–1679

Authors' addresses: Harri Koivusalo (e-mail: hkoivusa@water.hut.fi), T. Karvonen, Laboratory of Water Resources, Helsinki University of Technology, P.O. Box 5200, FIN-02015 HUT, Finland; M. Heikinheimo, Finnish Meteorological Institute, P.O. Box 503, FIN-00101 Helsinki, Finland.